Enhanced UV emission from ZnO nanoflowers synthesized by the hydrothermal process



2012 J. Phys. D: Appl. Phys. 45 425103

(http://iopscience.iop.org/0022-3727/45/42/425103)

IOP Publishing Journal of Physics D: Applied Physics
J. Phys. D: Appl. Phys. **45** (2012) 425103 (6pp) doi:10.1088/0022-3727/45/42/425103

# Enhanced UV emission from ZnO nanoflowers synthesized by the hydrothermal process

**R Vinod[1], P Sajan[1], Sreekumar Rajappan Achary[2], Carmen Martinez Tomas[2], Vicente Muñoz-Sanjosé[2] and M Junaid Bushiri[1]**

[1] Department of Physics, Cochin University of Science and Technology, Kochi 682022, Kerala, India
[2] Departamento de Fisica Aplicada y Electromagnetismo, Universitat de Valencia, c/Dr Moliner 50, Burjassot, Valencia 46100, Spain

E-mail: junaidbushiri@gmail.com

Received 11 June 2012, in final form 9 August 2012
Published 4 October 2012
Online at stacks.iop.org/JPhysD/45/425103

**Abstract**
ZnO nanoflowers were synthesized by the hydrothermal process at an optimized growth temperature of 200 °C and a growth/reaction time of 3 h. As-prepared ZnO nanoflowers were characterized by x-ray diffraction, scanning electron microscopy, UV–visible and Raman spectroscopy. X-ray diffraction and Raman studies reveal that the as-synthesized flower-like ZnO nanostructures are highly crystalline with a hexagonal wurtzite phase preferentially oriented along the (1 0 $\bar{1}$ 1) plane. The average length (234–347 nm) and diameter (77–106 nm) of the nanorods constituting the flower-like structure are estimated using scanning electron microscopy studies. The band gap of ZnO nanoflowers is estimated as 3.23 eV, the lowering of band gap is attributed to the flower-like surface morphology and microstructure of ZnO. Room temperature photoluminescence spectrum shows a strong UV emission peak at 392 nm, with a suppressed visible emission related to the defect states, indicating the defect free formation of ZnO nanoflowers that can be potentially used for UV light-emitting devices. The suppressed Raman bands at 541 and 583 $cm^{-1}$ related to defect states in ZnO confirms that the ZnO nanoflowers here obtained have a reduced presence of defects.

## 1. Introduction

ZnO is a wide band gap (3.37 eV) transparent semiconductor material with attractive technological applications [1]. ZnO is a potential photocatalyst, has the advantage of lower cost, absorbing more light quanta and higher photocatalytic efficiencies for the degradation of several organic pollutants in both acidic and basic medium than $TiO_2$ [2]. ZnO is also a promising material for short wavelength optoelectronic devices, especially UV light-emitting diodes, LEDs and laser diodes due to its large exciton binding energy (60 meV) [3]. The preparation of crystalline ZnO with specific structures is crucial to explore its potential applications in depth [4]. ZnO nanostructures with different morphologies, such as flower-like [5], nanorods [6], nanowires [7], nanobridges, nanonails [8], nano/micro-sized particles [9] and micro-tubes [10] can be synthesized by different methods. These nanostructures can be used as efficient gas sensors and also for the fabrication of photodiodes, photodetectors, solar cells and next generation UV sources [11]. ZnO nanostructures usually exhibit UV near band-edge (NBE) emission as well as defect level emission in the visible region [12]. Light-emitting properties and photocatalytic activity of ZnO nanostructures can be modified by changing its structural and morphological features [13]. It is a technologically important and challenging task to synthesize ZnO nanostructures at low cost to be used as UV generating sources. In this context, hydrothermal synthesis is a promising eco-friendly solution based method to grow different types of ZnO nanostructures. It is worth noting that Haiyong *et al* have demonstrated the ability of a direct growth of ZnO nanoflowers on substrates using the hydrothermal method: GaN-based LED epiwafer and AlN that are grown on c-sapphire [14, 15].

 

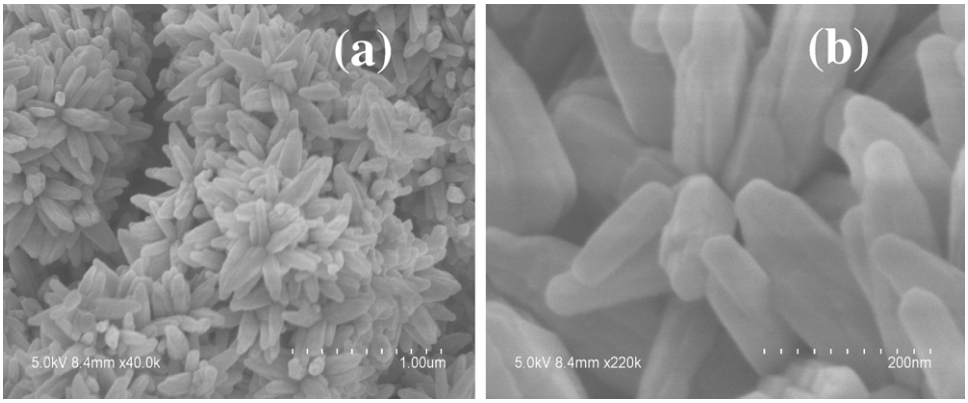


**Figure 1.** SEM images of (*a*) ZnO nanoflowers synthesized by the hydrothermal method and (*b*) is a magnified image of the same sample.

Recently, flower-like ZnO nanostructures were identified to be a material of choice for fabricating low power consumption sensors because of its respond time (about 30 s) longer than that for sensors working at high temperatures [16]. Flower-like ZnO nanostructures (ZnO nanoflowers) proved their potential use as photoanode for dye-sensitized solar cells that enhanced the solar cell efficiency about 90% due to improved dye-loading and light harvesting [17]. On the other hand, Kim *et al* [18] studied the field emission characteristics of the flower-like ZnO arrays for cold cathode emitter applications. ZnO nanoflowers exhibited excellent electron emission characteristics with a low turn-on field of 0.13 V $\mu$m$^{-1}$ which was several orders of magnitude lower than that of 7.6 V $\mu$m$^{-1}$ for the vertically aligned high-density ZnO nanoneedles [18]. Furthermore, the light-emitting devices fabricated using these nanoflowers arrays as electron emitter demonstrated strong light emission, indicating that the luminescence originates from the electron emission from the ZnO nanoflower arrays. There are many studies reported on the growth of ZnO nanoflowers with a growth temperature ranging from 90 to 200 °C and reaction/growth time of 30 min to 13 h [14, 15, 19–21]. The reduction in reaction time is an important consideration with respect to a large scale production of nanomaterials for technological applications. However, in all the above-mentioned studies the ZnO nanoflowers exhibited the un-desirable green/visible emission related to the defect states in the ZnO nanostructures. Taking this into account, we have performed several experiments in order to optimize the growth condition of ZnO nanoflowers by a hydrothermal synthesis process with a short reaction time and low growth temperature in order to obtain flower-like ZnO nanostructures with minimum defect related emission. In this work, we report the synthesis and characterization of ZnO nanoflowers with enhanced UV emitting nature (with suppressed visible emission related to defect states in ZnO), grown by the hydrothermal method at an optimized growth temperature of 200 °C and a growth time of 3 h.

## 2. Experimental

ZnO nanoflowers were synthesized by the reaction of $Zn(CH_3COO)_2.2H_2O$ (0.1M) and NaOH (1M) under autogenous pressure, at a temperature of 200 °C for a growth time of 3 h. The pH of the reaction solution was about 8–10. The entire reaction was carried out in a teflon lined sealed stainless-steel autoclave. After the heating process, the autoclave was allowed to cool naturally to room temperature. As-collected resulting white precipitate was washed with distilled water, filtered and dried in air atmosphere at room temperature. The structural characterization of synthesized samples was carried out by a Rigaku (D.Max.C) x-ray diffractometer and a high resolution (HR) PANalytical X'Pert Materials Research four-circle Diffractometer (MRD), both using Cu K$\alpha$ radiation ($\lambda$ = 1.5414 Å). The HR diffractometer was provided with optics for the incident beam which had a 4-bounce hybrid monochromator, ensuring an output collimated beam to about 18 arcsec in the plane of scattering. A scanning rate in the order of 0.0012° s$^{-1}$ was used to record the diffraction pattern using the HR diffractometer. The morphological characterization of the sample was carried out using a Hitachi S-4800 scanning electron microscope (SEM). Raman spectrum of the sample was recorded with a Horiba Jobin Yvon Lab Ram HR system with Ar-ion laser (514.5 nm) as the excitation source with a resolution better than 3 cm$^{-1}$. The UV–visible spectrum was recorded within the wavelength range 200–800 nm with a Jasco V-570 spectrometer. Room temperature photoluminescence (PL) of the samples was measured on a Horiba Jobin Yvon LabRam HR system with the He–Cd laser (325 nm) as excitation source.

## 3. Results and discussion

Figure 1 depicts the SEM images of the ZnO nanoflowers synthesized at an optimized growth temperature of 200 °C and a growth time 3 h. The morphology of the ZnO nanoflowers here obtained closely matched with that obtained by Zhang *et al* [22] using the hydrothermal process and Chu *et al* using the solution growth process [21]. The average length and diameter of the nanorods constituting the ZnO nanoflowers were estimated to be about 234–347 nm and 77–106 nm, respectively. SEM images recorded from various regions of the sample exhibited the uniform morphology. The x-ray diffraction patterns/peaks recorded from the ZnO nanoflowers are indexed according to the typical hexagonal wurtzite structure of ZnO with space group $P63mc$ (JCPDS: 36-1451)

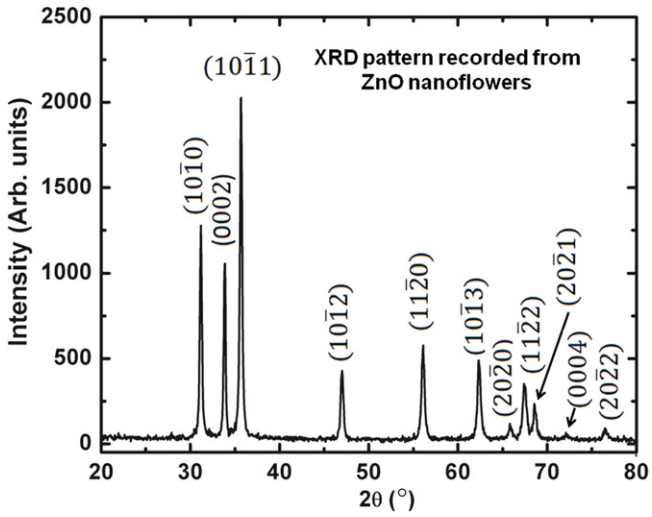


**Figure 2.** X-ray diffraction pattern of ZnO nanoflowers.

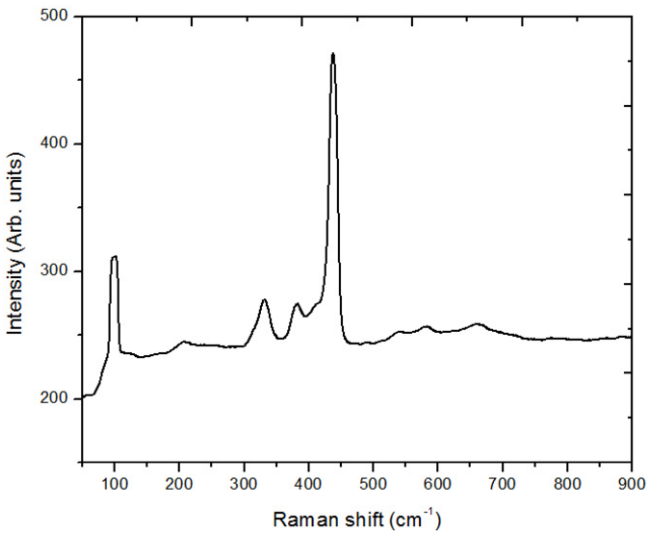


**Figure 3.** Raman spectrum of ZnO nanoflowers synthesized by the hydrothermal method.

(figure 2). The sample exhibited preferential orientation along the (1 0 $\bar{1}$ 1)plane. However, we can observe sharp diffraction peaks from the (1 0 $\bar{1}$ 0) and (0 0 0 2)plane indicating the good crystallinity and purity of the prepared sample. The x-ray diffraction peak along the (0 0 0 2)plane is indicative that growth of ZnO nanorods constituting the ZnO nanoflowers is in the *c*-axis orientation. The lattice parameters have been obtained from Bragg's law and from HR $2\theta$-$\theta$ spectra [23]. After a fine calibration of the $2\theta$ position, appropriate reflections at high angles have been chosen in order to obtain a low error. From the distance between planes obtained for symmetrical reflections ($d_{0004}$ and $d_{0006}$) the '*c*' parameter has been determined directly. Next, using this value, the parameter '*a*' has been calculated from the distance between planes of high angle asymmetrical reflections ($d_{21\bar{3}3}$, $d_{30\bar{3}2}$, $d_{20\bar{2}5}$). The low divergence of the collimated beam assures a relative error lower than 0.3%. The values so obtained are $a = 3.2491$ Å and $c = 5.2151$ Å. These values are slightly different from the standard values of hexagonal ZnO: $a = 3.2498$ Å and $c = 5.2066$ Å (JCPDS: 36-1451). The differences here observed from ZnO nanoflowers can be due to the surface stress on the nanostructures. This stress induces a lattice strain, leading to a lattice expansion, mainly in the *c*-direction, in order to relieve the strain [24]. We can consider this as evidence that in ZnO nanoflowers grown using the hydrothermal process, the stress relaxes elastically.

The catalyst free growth of ZnO nanoflowers at low temperature depends on the other growth conditions. The physical and chemical nature of the solvents is the key factor which influences the nucleation and the oriented growth process of ZnO materials [25]. The reaction between $Zn(CH_3COO)_2.2H_2O$ and NaOH will give $Zn(OH)_2$ which is not stable with a heat treatment under autogenous pressure. Therefore, $Zn(OH)_2$ dissociates to $Zn^{2+}$ ions and $OH^-$ ions, and the detachment of $OH^-$ radical may activate the nucleation centres. ZnO nuclei can be preferentially formed on the coalescent sites by the Coulomb interactions between $Zn^{2+}$ ions and $O^-$ ions within the solution [22]. As the time of growth increases more ZnO molecules will be attached to the initially formed nucleation centres. On these individually formed nucleation centres, bundles of ZnO nanorods are aggregated in three-dimensional-array and flower-like morphology is developed.

**Table 1.** Raman active phonon mode frequencies (in cm$^{-1}$) and process compared with single crystal ZnO.

| Frequency (cm$^{-1}$) | | |
|---|---|---|
| This work (Nanoflowers) | Single crystal ZnO [26] | Process |
| 99 (s) | 99 | $E_2^{low}$ |
| 330 (w) | 333 | $E_2^{high}$–$E_2^{low}$ |
| 382 (w) | 378 | A1(TO) |
| 437 (vs) | 438 | $E_2^{high}$ |
| 541 (vw) | 536 | $2B_1^{low}$; 2LA |
| 583 (vw) | 590 | $E_1$(LO) |

*Note*: w: weak, vw: very weak, vs: very strong, s: strong.

Raman spectroscopy is one of the tools to determine the crystallinity and/or the quality of semiconductor crystals. Figure 3 depicts the Raman spectrum recorded from the ZnO nanoflowers. In the Raman spectrum of the sample, a strong Raman active phonon band located at 437 cm$^{-1}$ corresponds to $E_2^{high}$ mode, whereas the suppressed bands of ZnO observed at 583 and 541 cm$^{-1}$ are attributed to the $E_1$(LO) mode and second order $2B_1^{low}$; 2LA overtones, respectively, [26, 27]. The presence of an intense $E_2^{high}$ mode and a suppressed $E_1$(LO) mode in the Raman spectrum indicates that the as-synthesized ZnO nanoflowers are highly crystalline with a hexagonal wurtzite phase which is in agreement with x-ray diffraction results. Another three prominent Raman modes are observed at 99, 330 and 382 cm$^{-1}$. Raman bands recorded from the ZnO nanoflowers are compared with the reported values of single crystal ZnO which are presented in table 1 [26]. The strong band observed $E_2$ (high) at 437 cm$^{-1}$ is the intrinsic characteristic Raman active mode of wurtzite hexagonal ZnO [28]. The Raman bands at 99 cm$^{-1}$, 330 cm$^{-1}$ and 382 cm$^{-1}$ [26] corresponds to multiple phonon scattering processes of $E_2$ (low), $E_2^{high}$–$E_2^{low}$ and $A_1$(TO) modes, respectively.

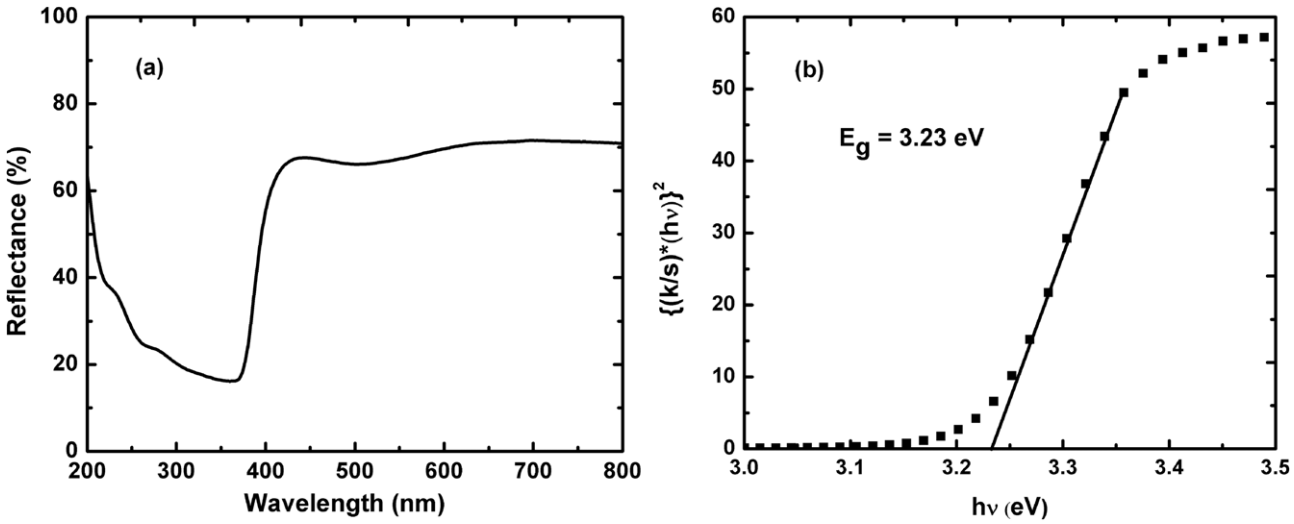


**Figure 4.** (*a*) Reflectance spectrum and (*b*) $\{(k/s)h\nu\}^2$ versus $h\nu$ plot of ZnO nanoflowers synthesized by the hydrothermal method.

Raman peaks observed in between 541 and 583 $cm^{-1}$ are associated with structural disorders, such as oxygen vacancy, Zn interstitial and their combination [29–31]. It is to be noted that the Raman modes correspond to defect states (541 and 583 $cm^{-1}$) are very weak, pointing to the fact that the ZnO nanostructure obtained here, using the hydrothermal process are with comparatively less number of optical active defects, which we will demonstrate in the following section using the PL study.

Figure 4(*a*) depicts the reflectance spectrum recorded from ZnO nanoflowers. The optical absorption edge of ZnO nanoflowers appears at 384 nm which is red shifted by 11 nm relative to the bulk exciton absorption (373 nm) [32]. Correspondingly, the ZnO nanoflowers exhibited a lower optical energy gap of 3.23 eV with respect to bulk ZnO. The band gap of the flower-like ZnO nanostructure is estimated from $\{(k/s)h\nu\}^2$ versus $h\nu$ plot (figure 4(*b*)), where $k$ and $s$ denote the absorption and scattering coefficients, respectively, and $h\nu$ is the photon energy [33]. The ratio of $(k/s)$ is calculated from the reflectance via the Kubelka–Munk equation [34]. The reason for red shift in absorption edge/optical energy gap can be well explained as due to the oriented attachment of the nanorods and it has been specifically observed in ZnO with flower-like morphology [4]. Using x-ray diffraction analysis we have seen that ZnO nanoflowers obtained using the hydrothermal process are strain relaxed, as evident from the enhanced lattice parameters '*a*' and '*c*'. This in turn could incur a slight decrease in the band gap of the ZnO nanoflowers [35].

The room temperature PL spectrum under the excited wavelength of 325 nm of the as-prepared ZnO nanoflowers is shown in figure 5. The PL spectrum of the ZnO nanoflowers generally shows two emission bands, one is in the UV region at 392 nm, and an almost negligible blue band at 510–580 nm. The UV emission band at 392 nm pertains to the recombination of free excitons between the conduction and valence bands and is called the NBE emission (NBE), while the longer wavelength band can be attributed to the radial recombination of a photo-generated hole with electron, which belongs to

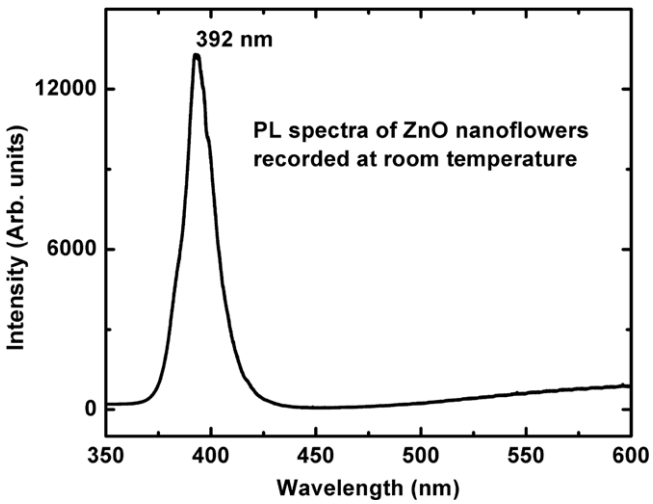


**Figure 5.** PL spectrum of ZnO nanoflowers at room temperature.

the singly ionized oxygen vacancy [36]. The strong UV emission located at 392 nm in the PL spectrum of the present sample indicates that the ZnO nanoflowers have good crystal quality with few oxygen vacancies which corresponds to the self-activated luminescence [28]. The improvement in the crystal quality such as low structural defects, oxygen vacancies, zinc interstitials and decrease in the impurities may cause the appearance of sharper and stronger UV emission and a suppressed and weakened green and red emission [37]. Moreover, the optical properties are also directly influenced by the morphologies and size of the final products [38]. The structure of flower-like ZnO has small size and large surface area which in turn contributes to intensity enhancement.

Chu *et al* [21], in a study conducted on ZnO nanoflowers grown using the solution growth technique, observed an enhanced visible emission centred around ∼550 nm over the UV emission with an increase in the random distribution of ZnO nanoflowers. The dominant visible emission observed (with respect to the UV emission) was explained due to the enhanced adsorbed oxygen as a result of increased surface area

of the random distributed ZnO nanoflowers. Similarly they observed a gradual decrease in the x-ray diffraction peak along the (0 0 0 2)plane with increase in the random distribution of ZnO nanoflowers, which is evidence of degradation of the *c*-axis orientation of the ZnO nanorods constituting the flowers [21]. In our case we obtained randomly distributed ZnO nanoflowers morphology similar to that obtained by Chu *et al* [21]. However, our ZnO nanoflowers exhibited negligible visible emission related to the defect states as compared with the UV emission centered at 392 nm. The x-ray diffraction pattern recorded from ZnO nanoflowers exhibited strong and sharp peak of ZnO along the (0002)plane (figure 2). This indicates that even though the ZnO nanoflowers are randomly distributed, the ZnO nanorods constituting the nanoflowers structure are well oriented in the *c*-axis orientation, which favours the growth of ZnO nanoflowers with minimal defects (adsorbed oxygen, oxygen vacancy, Zn interstitial). Similarly Raman analysis supported our claim that the ZnO nanoflowers have minimum defect states, as observed from the suppressed Raman active modes at 541 $cm^{-1}$ and 583 $cm^{-1}$, respectively.

## 4. Summary and conclusions

In summary, good crystalline ZnO nanoflowers with significant reduction in the presence of optical active defects can be synthesized by a low-temperature hydrothermal method at a relatively low reaction time of 3 h. The x-ray diffraction and Raman analysis confirmed the crystalline quality of the ZnO nanoflowers. HR x-ray diffraction measurements reveal that stress relaxes elastically in ZnO nanoflowers grown using the hydrothermal process. This behaviour is determined from the calculation of lattice parameters which indicate an expansion, mainly in the *c*-direction, of the ZnO nanoflowers. ZnO nanoflowers exhibited an optical energy gap of 3.23 eV, the lower band gap value (with respect to the bulk ZnO) obtained is explained as a result of flower-like surface morphology and the expansion of lattice in order to relieve the lattice strain. The room temperature PL spectrum of ZnO nanoflowers shows a strong UV emission peak at 392 nm with a negligible visible emission related to the defect states as compared with the UV emission. The very weak Raman active modes at 541 and 583 $cm^{-1}$ associated with the defect states in ZnO confirm the significant reduction of the optical active defects. Therefore, the ZnO nanoflowers grown using the hydrothermal process at an optimized growth temperature and growth time can be used as a good UV emitting source in light-emitting devices.

## Acknowledgments

R Vinod acknowledges University Grants Commission, Government of India, for research fellowship. The authors acknowledge Professor M K Jayaraj, Nanophotonic and Optoelectronic Devices laboratory, Department of Physics, CUSAT, for providing Raman measurements under Department of science and Technology nanomission initiative programme. The authors are grateful to the Central Support Service in Experimental Research (SCSIE), University of Valencia, Spain, for providing SEM and HRXRD facilities. This work was partially supported by the Spanish Ministry of Science and Innovation and EU-FEDER under projects MAT2007-66129 and TEC2011-28076-C02-02 and Generalitat Valenciana through the projects Prometeo/2011-035 and ISIC/2012/008 (Institute of Nanotechnologies for Clean Energies of the Generalitat Valenciana).

## References

[1] Reynolds D C, Look D C, Jogai B, Hoelscher J E, Sherriff R E, Harris M T and Callahan M J 2000 *J. Appl. Phys.* **88** 2152
[2] Yang L Y, Dong S Y, Sun J H, Feng J L, Wu Q H and Sun S P 2010 *J. Hazardous Mater.* **179** 438
[3] Huang M H, Mao S, Feick H, Yan H Q, Wuand Y Y, Kind H, Weber E, Russo R and Yang P D 2001 *Science* **292** 1897
[4] Yang W, Li Q, Gao S and Shang J K 2011 *Nanoscale Res. Lett.* **6** 491
[5] Pal U and Santiago P 2005 *J. Phys. Chem.* B **109** 15317
[6] Tak Y and Yong K 2005 *J. Phys. Chem.* B **109** 19263
[7] Yang P, Yan H, Mao S, Russo R, Johnson J, Saykally R, Morris N, Pham J, Rongrui H and Choi H J 2002 *Adv. Funct. Mater.* **12** 323
[8] Lao J, Huang J, Wang D and Ren Z 2003 *Nano Lett.* **3** 235
[9] Mc Bride R A, Kelly J M and Mc Cormack D E 2003 *J. Mater. Chem.* **13** 1196
[10] Vayssieres L, Keis K, Hagfeldt A and Lindquist S E 2001 *Chem. Mater.* **13** 4395
[11] Baruah S and Dutta J 2009 *Sci. Tecnol. Adv. Mater.* **10** 013001
[12] Ko Y H, Kim M S and Yu J S 2012 *Nanoscale Res. Lett.* **7** 13
[13] Zhang Y, Zhang W and Zheng H 2007 *Scr. Mater.* **57** 313
[14] Haiyong G, Fawang Y, Jinmin L, Yiping Z and Junxi W 2007 *J. Phys. D: Appl. Phys.* **40** 3654
[15] Haiyong G, Fawang Y, Zhang Y, Jinmin L and Yiping Z 2008 *Chin. Phys. Lett.* **25** 640
[16] Chen Y, Zhu C L and Xiao G 2006 *Nanotechnology* **17** 4537
[17] Jiang C Y, Sun X W, Lo G Q and Kwong D L 2007 *Appl. Phys. Lett.* **90** 263501
[18] Yong J K, Jinkyoung Y, Byoung H K,Young J H, Chul H L and Gyu-Chul Yi 2008 *Nanotechnology* **19** 315202
[19] Yuxin W, Xinyong L, Ning W, Xie Q and Yongying C 2008 *Separation Purification Technol.* **62** 727
[20] Jiechao G, Bo T, Linhai Z and Zhiqiang S 2006 *Nanotechnology* **17** 1316
[21] Chu D, Yoshitake M, Tatsuki O and Kazumi K 2010 *J. Am. Ceram. Soc.* **93** 887
[22] Zhang H, Yang D, Ma X, Ji Y, Xu J and Que D 2004 *Nanotechnology* **15** 622
[23] Moram M A and Vickers M E 2009 *Rep. Prog. Phys.* **72** 036502
[24] Sameer D, Swanand P, Satyanarayana V N T K and Sudipta S 2005 *Appl. Phys. Lett.* **87** 133113
[25] Zhang R, Yang X, Zhang D, Qin J, Lu C, Ding H, Yan X, Tang H, Wang M and Zhang Q 2011 *Cryst. Res. Technol.* **46** 1189
[26] Ramon C, Esther L, Jordi I, Luis A, Juan J, Buguo W and Michael J C 2007 *Phys. Rev.* B **75** 165202
[27] Pal U, Garcia S J, Santiago P, Gang X, Ucer K B and Williams R T 2006 *Opt. Mater.* **29** 65
[28] Rajalakshmi M, Arora A K, Bendre B S and Mahamuni S 2000 *J. Appl. Phys.* **87** 2445
[29] Rizwan W, Ansari S G, Kim Y S, Seo H K, Kim G S, Khang G and Shin S S 2007 *Mater. Res. Bull.* **42** 1640
[30] Decremps F, Porres J P, Saitta A M, Chervin J C and Polian A 2002 *Phys. Rev.* B **65** 92101
[31] Chen Z Q, Kawasuso A, Xu Y, Naramoto H, Yuan X L, Sekiguchi T, Suzuki R and Ohdaira T 2005 *Phys. Rev.* B **71** 115213

[32] Haase M, Weller H and Henglein A 1998 *J. Phy. Chem.* **92** 482
[33] Kubelka P and Munk F 1931 *Z. Tech. Phys.* **12** 593
[34] Omata T, Ueda N, Ueda K and Kawazoe H 1994 *Appl. Phys. Lett.* **64** 1077
[35] Kim K S, Jeong H, Jeong M S and Jung G Y 2010 *Adv. Funct. Mater.* **20** 3055
[36] Gao S, Zhang H, Wang X, Deng R, Sun D and Zheng G 2006 *J. Phys. Chem.* B **110** 15847
[37] Bagnall D M, Chen Y F, Zhu Z, Yao T, Shen M Y and Goto T 1998 *Appl. Phys. Lett.* **73** 1038
[38] Wu R, Yang Y, Cong S, Wu Z, Xie C, Usui H, Kawaguchi K and Koshizaki N 2005 *Chem. Phys. Lett.* **406** 457